HHS Public Access

Author manuscript

Toxicol In Vitro. Author manuscript; available in PMC 2022 August 23.

Published in final edited form as:

Toxicol In Vitro. 2011 June ; 25(4): 774–784. doi:10.1016/j.tiv.2011.01.013.

A critical analysis of single-frequency LCR databridge impedance measurements of human skin

Erick A. White[a], **Mark E. Orazem**[b], **Annette L. Bunge**[a,*]

[a]Chemical Engineering Department, Colorado School of Mines, Golden, CO 80401, USA

[b]Chemical Engineering Department, University of Florida, Gainesville, FL 32611, USA

Abstract

Testing whether the barrier of skin samples has sufficient integrity for meaningful measurements of *in-vitro* chemical permeability is usually required when data are generated for regulatory purposes. Recently, skin integrity has been assessed using LCR databridge measurements, which are reported as resistances determined in either series (SER) or parallel (PAR) modes at a single frequency, typically 100 or 1000 Hz. Measurements made at different combinations of mode and frequency are known to differ, although the skin literature reveals confusion over the meaning of these differences and the impact on the interpretation of integrity test results. Here, the theoretical meanings of resistance and capacitance measurements in PAR and SER mode are described and confirmed experimentally. SER-mode resistances are equal to the real part of the complex impedance; whereas, PAR-mode resistances are the inverse of the real part of the admittance. Capacitance measurements reported in SER and PAR modes are similar manipulations of the imaginary parts of the complex impedance and admittance. A large body of data from human cadaver skin is used to show that the PAR-mode resistance and SER-mode capacitance measured at 100 Hz are sensitive to skin resistivity, which is the electrical measurement most closely related to skin integrity.

Keywords

Electrical impedance spectroscopy; Skin barrier function; Stratum corneum; Skin integrity; *In-vitro* ; Constant phase element

1. Introduction

Measurement of electrochemical impedance has been shown to be a convenient method for characterizing many different materials, including human or animal skin. The method involves applying small-amplitude sinusoidal modulation of an input current or potential and measuring the responding potential or current. Impedance is the ratio of the change in potential to the change in current. Because the phase difference between the measured and input signals depends on the modulation frequency, it is convenient to express the impedance as a complex number that varies with the frequency of the time variation. In the limit of low

*Corresponding author. Address: Colorado School of Mines, Chemical Engineering Department, 1500 Illinois Street, Golden, CO 80401-1887, USA. Tel.: +1 303 273 3722; fax: +1 303 273 3730., abunge@mines.edu (A.L. Bunge).

frequency, the impedance measurement should approach the direct current (DC) resistance (R_{DC}).

Percutaneous absorption data are required for risk assessments of potentially toxic chemicals. *In-vitro* measurements of human skin can be used to avoid testing on human volunteers or animals. However, the collection and handling of excised skin can introduce damage, which may affect the percutaneous absorption measurements (Scott et al., 1991). Therefore, testing whether the barrier function of skin samples has sufficient integrity for meaningful measurements of *in-vitro* chemical permeability is common and usually required when data are generated for regulatory purposes (Heylings and Esdaile, 2007; International Programme on Chemical Safety (IPCS), 2006; OECD, 2004a). Measurement of skin impedance is faster and less expensive than measuring tritiated water permeation (Davies et al., 2004; Fasano and Hinderliter, 2004; Fasano et al., 2002), which has been the conventional skin integrity test (Franz and Lehman, 1990; Kasting et al., 1994; Scott et al., 1992). For the same reason, *in-vitro* impedance measurements are also used to identify chemicals and chemical mixtures that cause irreversible (or corrosive) damage to the skin (OECD, 2004a).

Several papers have described impedance measurements of *in-vitro* skin samples determined using an LCR databridge; e.g., from PRISM (Davies et al., 2004; OECD, 2004b) or Tinsley (Fasano et al., 2002). According to their manufacturers, these instruments measure inductance (L), capacitance (C) or resistance (R) in either a parallel (PAR) or series (SER) mode determined at one of two user-selected frequencies, usually 100 or 1000 Hz. Nearly always, the reported resistance values measured by PAR and SER modes (i.e., R_{PAR} and R_{SER}, respectively) at a given frequency are different. Also, R_{PAR} and R_{SER}, determined at different frequencies, are different, clearly indicating that these instruments are not reporting the DC skin resistance (Fasano and Hinderliter, 2004).

In assessing skin integrity or corrosion, the meaningful quantity is the electrical resistivity of the skin (ρ), which quantitatively characterizes the pathway for transport of ions. Consistent with this, the permeability of polar and ionic chemicals through skin has been shown to be inversely proportional to the resistivity (Kasting and Bowman, 1990; Peck et al., 1994, 1995). Low resistivity, therefore, indicates high permeability to ions or polar chemicals, which is consistent with damage. Because the thickness of the stratum corneum (l), the skin layer primarily responsible for electrical resistance, is not usually measured, it is convenient to report the product of ρ and l, which is equal to the DC resistance of the skin (R_{skin}) multiplied by the area for charge transfer (A). LCR databridge measurements of skin will meaningfully assess skin integrity or damage only if the resistance measured represents a reliable estimate of the DC resistance.

The strategy is to reject skin samples with resistivity below a specified acceptance criterion as being too damaged for determining reliable chemical permeation parameters. Typically, the acceptance criterion is selected by comparing electrical measurements on a series of samples to the percutaneous absorption measurements for tritiated water (Davies et al., 2004; Fasano et al., 2002), other polar compounds (Peck et al., 1995), or ionized salts (Kasting and Bowman, 1990). Peck et al. (1995) and Kasting and Bowman (1990)

recommended that DC resistance values of 20 and 35 kΩ cm^2, respectively, were suitable acceptance criteria. Proposed minimum acceptable values in R_{PAR} from LCR databridge measurements, derived by comparing R_{PAR} measurements to the same maximum acceptable tritiated water absorption of 1.5 mg cm^{-2} h^{-1} (which is equal to a permeability coefficient of 1.5×10^{-3} cm/h), differ depending on the frequency of the R_{PAR} measurement. Fasano et al. (2002) suggested that skin samples be rejected if they have a resistance, measured at 1000 Hz and normalized for area, less than 11 kΩ cm^2. Davies et al. (2004) recommended using a criterion of 25 kΩ cm^2 based on measurements at 100 Hz. (Note that Davies et al. (2004) incorrectly listed the measuring frequency as 100 kHz rather than 100 Hz (Heylings, 2009).) The OECD 430 guidelines for identifying corrosive chemicals used measurements at 100 Hz in SER mode in validation studies, and recommend measurement frequencies between 50 and 1000 Hz (OECD, 2004b).

Given that skin integrity is characterized by the resistivity, equal to R_{skin} A/l, it is important to know the extent to which LCR databridge measurements at 100 or 1000 Hz, reported in either PAR or SER modes, are correlated with the DC skin resistance. The objective of this work is to explain and establish experimentally the electrical quantities represented by R_{PAR} and R_{SER} and also the capacitance reported in PAR and SER modes (i.e., C_{PAR} and C_{SER}, respectively). A large quantity of skin impedance data is used to demonstrate the significant advantage of using the PAR resistance measurements at 100 Hz or the SER capacitance measurements at 100 Hz to estimate the skin resistivity, and therefore, integrity. These data are also used to derive equations relating the DC resistance to R_{PAR} at 100 and 1000 Hz and C_{SER} at 100 Hz. In a companion study, measurements of tritiated water permeation are shown to be linearly correlated with estimates of DC resistance derived from LCR databridge measurements determined at either 100 or 1000 Hz in three different laboratories (White, 2011).

2. Theory

Impedance (Z) is the alternating current (AC) analog to the DC resistance (R_{DC}), which is expressed in terms of real (Z_r) and imaginary (Z_j) parts as

$$Z = Z_r + jZ_j \tag{1}$$

where $j = \sqrt{-1}$. The inverse of the impedance is the admittance (Y), which is the AC analog of DC conductance. Like the impedance, the admittance can be written in terms of real (Y_r) and imaginary (Y_j) parts as

$$Y = \frac{1}{Z} = Y_r + jY_j \tag{2}$$

Notably, Z_r is only equal to the inverse of Y_r when the imaginary part of the impedance is zero.

The complex capacitance is defined to be the admittance (or the inverse of the impedance) divided by the angular frequency (ω), i.e.,

$$C = \frac{Y}{j\omega} = \frac{1}{jZ\omega} = C_r + jC_j \quad (3)$$

in which ω is equal to $2\pi f$, where f is the number of cycles per time. It is important to note that the complex capacitance depends on frequency and is not the intrinsic dielectric property of the material.

The presence of dielectric material in the skin causes a phase lag in the response to a periodic electrical signal. As a result, Z, Y and C measured for skin vary with frequency and include imaginary parts. It has been suggested that highly ordered stratum corneum lipids are the dielectric material (DeNuzzio and Berner, 1990; Oh et al., 1993). If skin were to behave as a simple resistor, there would be no phase shift and no imaginary parts, and Z and Y would be independent of frequency (Fasano and Hinderliter, 2004).

The references to ‘parallel’ and ‘series’ in the LCR databridge measurements is nomenclature from older technology in which a variable resistor and capacitor in either parallel or series circuits were used on one side of a Wheatstone bridge circuit. The electrochemical cell on which measurements are being made is connected to the other side of the Wheatstone bridge circuit, and the magnitudes of the capacitor and resistor are adjusted to balance the potential drop across the Wheatstone bridge. The values of the resistor and capacitor in the balanced circuit gave the real and imaginary parts of the impedance. If the configuration of the balancing circuit is a resistor and capacitor in series, then the impedance, referred to as Z_{SER} is given by:

$$Z_{SER} = R_{SER} + j\frac{-1}{\omega C_{SER}} = Z_r + jZ_j \quad (4)$$

It follows that the real part of the impedance, $Z_r = R_{SER}$, and the imaginary part of the impedance, $Z_j = -1/\omega C_{SER}$. Similarly, when the balancing circuit is configured as a resistor and capacitor in parallel, then the inverse of the impedance of the parallel circuit ($1/Z_{PAR}$) is equal to the inverse of the impedance for the resistor and capacitor as follows:

$$\frac{1}{Z_{PAR}} = Y_{PAR} = \frac{1}{R_{PAR}} + j\omega C_{PAR} = Y_r + jY_j \quad (5)$$

Therefore, the measured R_{PAR} is equivalent to $1/Y_r$ and the measured C_{PAR} is equivalent to Y_j/ω.

Unlike Wheatstone bridge devices, LCR databridge instruments do not contain an actual resistor–capacitor (R–C) measuring circuit. Instead, the LCR databridge instruments use a phase-sensitive analog-to-digital converter to determine the magnitude of the resulting voltage that is in-phase with the perturbation and the magnitude of the voltage that is out-of-phase with the perturbation. The corresponding current is measured with a current-to-voltage converter (H. Tinsley & Co., 1996). The measurement theory and practice is described in detail in the 6401 LCR Databridge Users Manual (H. Tinsley & Co., 1996).

A physical model of skin impedance is not available because the source of the skin impedance is not well understood. As a result, it is customary to use equivalent circuits, comprised of simple circuit elements, to model the skin impedance. A common circuit model of in-vitro skin impedance, depicted in Fig. 1, is a resistor that represents the frequency-independent (Ohmic) resistance containing contributions from the electrolyte, wires, and possibly the dermis (R_e) in series with a parallel resistor (R_{skin}) and capacitor (C_{skin}) that represent the skin polarization resistance and skin capacitance, respectively. Although this simple *R–C* circuit model does not represent actual skin impedance spectra as well as alternative circuit models like a resistor in parallel with a constant phase element (Hirschorn et al., 2010; Kontturi and Murtomaki, 1994; Yamamoto and Yamamoto, 1976a, 1976b, 1981), it is presented here because it does capture the important features.

The impedance response of the *R–C* circuit presented in Fig. 1 is similar to that of human skin, determined either *in-vitro* or *in vivo*, in that the Z_r in both cases approach asymptotic values at high and low frequencies. As the alternating current (AC) frequency approaches zero, Z_j approaches zero and Z_r approaches the DC resistance of the system; thus, $Z = Z_r = R_{DC} = R_e + R_{skin}$. For large frequencies, the impedance of the skin becomes negligibly small and $Z = Z_r = R_e$ (Orazem and Tribollet, 2008). The equations presented in Table 1 for R_{PAR}, R_{SER}, C_{PAR} and C_{SER}, corresponding to the *R–C* circuit in Fig. 1, can be obtained by algebraic rearrangements of the expressions describing the complex impedance provided in the Appendix. The equations describing R_{PAR}, R_{SER}, C_{PAR} and C_{SER} for a circuit with a resistor in series with a resistor in parallel with a constant phase element (*R*-CPE circuit) also are listed in the Appendix.

3. Materials and methods

Impedance and LCR databridge measurements were performed on a ‘‘dummy cell’’ circuit constructed of resistors and capacitors to confirm the interpretation of the LCR databridge results in terms of a full spectrum impedance analysis. Impedance measurements on human skin were then used to simulate LCR databridge readings and, thereby, to establish the relationship between LCR databridge measurements and skin integrity.

3.1. Dummy cell

A dummy cell electrical circuit, constructed to mimic approximately the impedance behavior of skin, was used to test the theoretical definitions of R_{PAR}, R_{SER}, C_{PAR} and C_{SER}. Specifically, measurements of R_{PAR}, R_{SER}, C_{PAR} and C_{SER} from an LCR databridge (Tinsley Model 6401 LCR Databridge, Croydon, UK) measured at 100 and 1000 Hz were compared to the complex impedance and admittance spectra determined for frequencies from 0.1 Hz to 20 kHz using a Gamry potentiostat (model PCI4/300, Warminster, PA). The dummy cell (Radio Shack, Fort Worth, TX) was assembled on a modular integrated circuit breadboard socket with a resistor ($R_e = 100 \pm 1\Omega$) placed in series with a second resistor ($R_{skin} = 115 \pm 1$ kΩ) that was in parallel with a capacitor ($C_{skin} = 47.0 \pm 9.4$ nF). The impedance electrode leads were connected to the circuit in a two electrode configuration with solderless breadboard jumper wires. The LCR databridge data were provided by C. Roper (Charles River Laboratories, Edinburgh, UK). For the Gamry

potentiostat measurements, the potential was modulated 10 mV rms with a mean applied potential of zero (i.e. no DC bias was applied) at 10 frequencies per logarithmic decade over the frequency range.

3.2. Chemicals and materials

Phosphate buffered saline (0.01 M) with 0.138 M NaCl, 0.0027 M KCl (pH 7.4, Sigma P-3813) was prepared in de-ionized (DI) water (Millipore Corporation, Bedford, MA). Split-thickness human cadaver skin (approximately 300 μm thick), harvested from the back or abdomen within 24 h post mortem, was purchased from National Disease Research Interchange (NDRI, Philadelphia, PA). The skin was immediately frozen after collection and stored at temperatures less than −60 °C until used.

3.3. Skin impedance

Impedance was measured across skin samples mounted between two horizontally oriented chambers in one of three configurations. Most experiments were conducted in glass Side-Bi-Side™ cells from PermeGear, Inc. (Hellertown, PA), which have an exposed skin area of 1.77 cm^2 and a 13-mL volume for each chamber. Other impedance experiments were conducted in custom-made, polycarbonate cells (0.64-cm^2 area and a chamber volume between 9 and 15 mL each), or in Side-Bi-Side™ cells modified to hold a customized frame assembly (PDM Services, Golden, CO), in which the skin is mounted (area and nominal volume are 1.70 ± 0.14 cm^2 and 13 mL, respectively). Both chambers of the three cell configurations were designed to accommodate two Ag/AgCl electrodes (*In Vivo* Metric, Healdsburg, CA), one working and one reference. The working electrodes were 12 mm diameter discs oriented with the face parallel to the skin surface. The cylindrical reference electrodes (1.5 mm diameter and 3 mm long) were oriented such that the long axis is parallel to the skin surface. During an experiment, both chambers were filled with PBS solution and the temperature was maintained at 32 °C in either a temperature-controlled environmental chamber (Electro-Tech Systems, Inc., PA) or by circulating water through the water jacket from a temperature-controlled bath.

Spectra of impedance–frequency scans were measured for 145 skin samples from six subjects (all Caucasian, four males, ages 51 to 78 years, average of 68.5 years) using the Gamry potentiostat at the same operating conditions used in the dummy cell experiment. The frequency range was from 1 Hz to 10 kHz, except for a few scans for which the frequency was as low as 0.1 Hz or as high as 300 kHz. Impedance scans were collected hourly during an equilibration period of 8–12 h to establish a baseline for the electrical properties of the skin as well as to verify that the skin was at equilibrium as indicated by insignificant differences between subsequent spectra. The frequency dependence in the measurements was consistent among the six subjects. No distinguishable effect of age or gender was observed; e.g., the subjects with the highest and lowest average impedance values (85 and 17 kΩ cm^2) were males of 78 and 76 years, respectively.

4. Results and discussion

Experiments performed on a ‘‘dummy cell’’ circuit constructed of resistors and capacitors provided confirmation of the relationship between LCR databridge values and impedance results at the same frequency. This correspondence was used to assess the use of LCR databridge values to estimate skin resistivity and as a measure of skin integrity.

4.1. Dummy cell measurements

Measurements of the dummy cell determined using the LCR databridge are compared in Fig. 2 to the Z_r and $1/Y_r$ spectra measured with the Gamry potentiostat. In agreement with the equations presented in Table 1, Z_r and $1/Y_r$ asymptotically approach the sum $R_e + R_{skin}$ at low frequency and R_e at high frequency. At intermediate frequencies, Z_r and $1/Y_r$ both decrease with frequency, although the rate of decrease for Z_r is greater than $1/Y_r$. Consistent with the definitions provided in Table 1 for LCR databridge measurements, values of R_{SER} measured at 100 Hz and 1000 Hz are indistinguishable from the corresponding Z_r values. Likewise, R_{PAR} measured at 100 Hz and 1000 Hz are indistinguishable from the corresponding $1/Y_r$ values.

Values for C_{PAR} and C_{SER} reported by the Tinsley 6401 at 100 Hz and 1000 Hz are compared in Fig. 3 to ($1/\omega Z_j$) and Y_j/ω calculated from the complex impedance spectra measured with the Gamry potentiostat. The values of C_{SER} and C_{PAR} determined at 100 Hz and 1000 Hz with the Tinsley instrument are indistinguishable from values of ($-1/\omega_j Z$) and Y_j/ω, respectively, which confirms the definitions of the C_{SER} and C_{PAR} measurements presented in Table 1. For an ideal R–C circuit, C_{skin} is the asymptotic limit for ($-1/\omega Z_j$) at high frequency and also for Y_j/ω at low frequency if $R_e << R$-$_{skin}$ (Table 1). For the dummy cell, the asymptotic limits of Y_j/ω and ($-1/\omega Z_j$) are the same and approximately 40 nF, which is within the component tolerance reported by the manufacturer. The small but evident frequency dependence at low and high frequency for Y_j/ω and ($-1/\omega Z_j$), respectively, indicates that the electrical components of the dummy cell were not perfectly ideal capacitors.

4.2. Application to human skin

The results presented in the previous section confirm that impedance measurements at 100 and 1000 Hz can be used to estimate the values of R_{PAR}, R_{SER}, C_{PAR}, and C_{SER} measured by a Tinsley LCR databridge. Values of R_{SER} and R_{PAR} calculated from the complex impedance measured as a function of frequency for two samples of human cadaver skin are presented in Fig. 4 as examples of skin exhibiting low and high impedance values. The frequency variation of C_{PAR} and C_{SER} are presented in Fig. 5 for the same two pieces of skin.

The features of the R_{SER} and R_{PAR} spectra for human skin are similar to those observed for the dummy R–C circuit shown in Fig. 2. At low frequency, R_{SER} and R_{PAR} asymptotically approach the DC resistance of the total cell (*i.e.,* $R_e + R_{skin}$), which is approximately 9 and 180 kΩ cm^2 for the low and high impedance samples, respectively. As with the dummy cell, R_{PAR} and R_{SER} both asymptotically approach R_e at higher frequencies. Also, like the

dummy cell, at a given intermediate frequency, R_{PAR} is larger than R_{SER} for both the high and low impedance skin. For both R_{SER} and R_{PAR}, the magnitude of any deviation from the DC resistance of the cell is reduced when measurements are made at lower frequency.

Notably, although the frequency dependence is similar for skin and the dummy cell, the maximum slope of the R_{PAR} and R_{SER} spectra is smaller for the skin samples than would be expected for an ideal R–C circuit. This is consistent with many other skin impedance studies (Hirschorn et al., 2010; Kontturi and Murtomaki, 1994; Membrino et al., 1997; Yamamoto and Yamamoto, 1976b), which found that, while the frequency dependence of the impedance for a simple R–C circuit model is similar to that measured in skin, a good quantitative fit of the skin data with an R–C circuit is not possible.

The C_{SER} and C_{PAR} spectra of the cadaver skin samples shown in Fig. 5 and the dummy cell shown in Fig. 3 also have similar features. The C_{PAR} spectra for the high and low impedance skin samples almost overlap, indicating little sensitivity to the large difference in DC resistance of the skin. Furthermore, the C_{PAR} values are nearly independent of frequency over most of the measured spectrum, decreasing significantly only at the higher frequencies. The rate of change of C_{SER} with frequency is large for both skin samples at frequencies less than about 100 Hz and relatively independent of frequency at frequencies of about 1000 Hz and higher. Overall, the C_{SER} spectra for the high impedance skin is shifted to the left relative to the C_{SER} spectra for low impedance skin, suggesting that C_{SER} is sensitive to variations in the DC cell resistance, although this will not be apparent if C_{SER} is measured at a higher frequency. At higher frequencies, C_{SER} for both pieces of skin approach a similar asymptotic value, which is related to, but not normally equal to, the effective capacitance of the skin sample (which is defined and discussed in the Appendix). Despite the more than 20-fold difference in the low frequency impedance values, the asymptotic values of C_{SER} at high frequency for the low and high impedance skin samples shown in Figs. 4 and 5 differ by only a factor of about two, which is consistent with the typically small variation in the effective capacitance for fully hydrated skin in diffusion cell experiments.

The frequency-dependent *in-vitro* measurements presented in Figs. 4 and 5 are consistent with measurements collected over a similar range of frequencies on human subjects *in vivo*, including the effects of treatments that caused skin damage; e.g., (Curdy et al., 2001, 2004; Kalia et al., 1996; Rosell et al., 1988). Quantitative *in-vitro*–*in-vivo* comparisons to these published data are not possible due to differences in the experimental protocols.

There are a few commercial instruments designed to assess human skin hydration *in vivo* through measurement of the total magnitude of the impedance, the reciprocal of the resistance of the impedance, or the capacitance contribution of the impedance (Barel and Clarys, 2006; Gabard et al., 2006; Nicander et al., 2006; Tagami, 2006). Quantitative comparisons of the measurements among these instruments are impossible due to differences in the measurement frequencies, the nature of the skin-electrode contact, and the electrode type, shape and configuration (Nicander et al., 2006). Compared with *in-vitro* impedance measurements, which are made across known skin layers, the skin depth measured by these commercial instruments is unknown and different for each. Also, some of the devices (e.g., the Corneometer from Courage-Khazaka Electronic) only report results

in arbitrary units related to skin hydration. Moreover, in contrast to the LCR databridge and Gamry measurements presented here, these commercial devices measure at frequencies that are large, at least 1 kHz and often greater than 1 MHz (Barel and Clarys, 2006; Gabard et al., 2006; Nicander et al., 2006; Tagami, 2006). Most probably the observations from these measurements are related to factors other than stratum corneum resistivity.

4.3. Estimation of skin resistivity

The resistance of skin is usually much larger than the Ohmic resistance (i.e., $R_{skin} >> R_e$), and, therefore, the low-frequency asymptote of the real part of the impedance approximates the DC resistance of the skin sample (R_{skin}). If the lowest frequency measured is sufficiently small, the low-frequency asymptote can be estimated by the real part of the impedance at the lowest frequency measured, designated as $Z_{r,lf}$. Values of R_{SER} and R_{PAR} calculated from the complex impedance measured at either 100 or 1000 Hz were normalized by $Z_{r,lf}$ for 145 samples of human cadaver skin. The corresponding ratios $R_{SER}/Z_{r,lf}$ and $R_{PAR}/Z_{r,lf}$ are presented in Fig. 6 as functions of R_{SER} and R_{PAR}, respectively. For all the samples shown in this and subsequent figures, the estimated difference between $Z_{r,lf}$ and the true value of R_{skin} is less than 4%.

Consistent with the results in Fig. 4 for two representative pieces of skin, the data presented in Fig. 6 show that R_{PAR} is a better estimate for $Z_{r,lf}$ than is R_{SER} at both frequencies (i.e., measurements of $R_{PAR}/Z_{r,lf}$ are close to 1 more often than are measurements of $R_{SER}/Z_{r,lf}$). Also, R_{PAR} more closely estimates $Z_{r,lf}$ when R_{PAR} is smaller; the same applies to R_{SER}. At 100 Hz, R_{PAR} and R_{SER} can underestimate $Z_{r,lf}$ by factors of 3 and 10, respectively. This increases to factors of 13 and 100 for R_{PAR} and R_{SER}, respectively when measured at 1000 Hz.

Overall, the skin impedance results shown in Fig. 6 indicate that skin resistivity and, therefore, its barrier function to ions or polar molecules is estimated better by impedance measurements at lower frequency, and that measurements at higher frequency may show little correlation with skin resistivity. This is consistent with observations from others. For example, Kalia et al. (1998) found that changes in measurements of *in vivo* transepidermal water loss (TEWL) during skin barrier function development in premature infants correlated with the modulus of the impedance measured at 1.6 Hz but not with impedance measured at 486 Hz. Also, in experiments comparing *in-vitro* measurements of tritiated water permeability with R_{PAR} determined at 1000 Hz for heat-separated human epidermal membranes, Fasano et al. (2002) observed that the natural logarithm of the tritiated water permeability was not linearly related to the natural logarithm of R_{PAR} measured at 1000 Hz. Their observation is consistent with the results presented in Fig. 6b and d, which shows that the ratios of $R_{PAR}/Z_{r,lf}$ and $R_{SER}/Z_{r,lf}$ measured at 1000 Hz were not equal to one or independent of the measured skin impedance.

The OECD guidelines for identifying chemicals that irreversibly damage skin recommend measuring impedance in SER mode at frequencies between 50 and 1000 Hz (OECD, 2004b). Based on the present, more thorough, examination of the frequency dependence of skin impedance measurements, the skin barrier to polar and ionic compounds is best assessed at a frequency that is not larger than 100 Hz.

Values of C_{SER}/A and C_{PAR}/A calculated from Gamry potentiostat measurements at 100 and 1000 Hz are presented in Fig. 7 as a function of ($Z_{r,lf}$ A) for the same skin samples shown in Fig. 6. As expected from the results shown in Fig. 5, C_{PAR} determined at either 100 or 1000 Hz is insensitive to variations in ($Z_{r,lf}$ A). In contrast, C_{SER} decreases with increasing $Z_{r,lf}$, although the data scatter for the measurements at 1000 Hz are too large to derive a meaningful correlation. However, measurements of C_{SER} at 100 Hz are obviously correlated with ($Z_{r,lf}$ A) with only a little scatter for skin samples having area-normalized values of $Z_{r,lf}$ between about 20 and 80 kΩ cm^2; for these, C_{SER}/A is related to ($Z_{r,lf}$ A) by

$$\log(C_{SER}/A) = -1.07\log(Z_{r,lf}A) + 3.85 \quad r2 = 0.94 \tag{6}$$

where the units for C_{SER}/A and ($Z_{r,lf}$ A) are nF/cm^2 and kΩ cm^2, respectively.

Two factors make C_{SER} measured at 100 Hz for human skin more sensitive to changes in the skin resistance than C_{SER} measured at 1000 Hz. First, the variation in the effective capacitance of most skin samples is relatively small. Second, 100 Hz is usually within a factor of about 4 of the characteristic frequency (f_c) for human skin, defined here as the frequency at which the negative of the imaginary component of the impedance is maximized. For an R– C model circuit, f_c is related to the skin resistance and capacitance as (Orazem and Tribollet, 2008):

$$f_c = \frac{1}{2\pi R_{skin} C_{skin}} \tag{7}$$

For an R-CPE circuit model, C_{skin} in Eq. (7) is the effective skin capacitance, $C_{skin,eff}$, which is described in the Appendix.

When C_{SER} is measured at a frequency close to the characteristic frequency, it varies strongly with R_{skin} but minimally with small variations in the effective skin capacitance. When measured at a frequency that is more than an order of magnitude larger or smaller than the characteristic frequency, C_{SER} is nearly insensitive to R_{skin} but affected by variations in the effective capacitance.

The variation of C_{SER} at 100 Hz and 1000 Hz with R_{skin} is illustrated in Fig. 8, in which predictions from the R-CPE model circuit (described by Eqs. (A7) and (A8) in the Appendix) are presented and compared to the 145 experimental values from Fig. 7. The model predictions were calculated at the mean value in the effective skin capacitance plus and minus one standard deviation assuming a log mean distribution of the effective capacitance values for the 145 skin samples shown in Figs. 6 and 7. Specifically, the mean ± one standard deviation in the logarithm of $C_{skin,eff}/A$ was equal to 1.60 ± 0.30, which corresponds to a mean of 39.8 nF/cm^2 with upper and lower bounds at 75.8 nF/cm^2 and 20.2 nF/cm^2, respectively. The α parameter in the R-CPE model was assumed to be 0.8, which is a typical number for skin (Hirschorn et al., 2009; Poon and Choy, 1981). The predicted dependence of C_{SER} with R_{skin} is in excellent agreement with the experimental results at both 100 and 1000 Hz.

The values of ($Z_{r,lf}$ A) at 20 and 80 kΩ cm^2 indicated on Fig. 8 designate the interval over which C_{SER} measured at 100 Hz appears to be approximately linear with ($Z_{r,lf}$ A). The characteristic frequencies for skin samples within the 20–80 kΩ cm^2 interval are approximately 25–400 Hz. For these samples, 100 Hz is within a factor of 4 smaller or larger than f_c, whereas, 1000 Hz is larger than f_c by 2.5 to 40-fold, which is consistent with the greater effect of skin resistance on C_{SER} measured at 100 Hz. Typically, f_c is less than 100 Hz for samples with (R_{skin} A) > 80 kΩ cm^2 and greater than 100 Hz for samples with (R_{skin} A) < 20 kΩ cm^2. Skin samples considered acceptable for diffusion cell determinations of chemical permeability generally have (R_{skin} A) that are 20 kΩ cm^2 or a little larger, which is within the approximately linear interval for C_{SER} and R_{skin}.

Interestingly, from the model predictions at 100 Hz (Fig. 8b) for a fixed effective skin capacitance, it is evident that C_{SER} actually is not linear with R_{skin} over the interval between 20 and 80 kΩ cm^2. The apparent linear relationship of C_{SER} and R_{skin} between 20 and 80 kΩ cm^2 is caused by the intersections of the C_{SER} versus R_{skin} curves at various values of the effective skin capacitance.

4.4. Application for assessing skin integrity

Often the goal of LCR databridge measurements is to test the integrity of skin samples used for *in-vitro* determinations of chemical permeation through skin. For this purpose, the meaningful test quantity is electrical resistivity, the magnitude of which, for LCR databridge instruments reporting R_{PAR}, R_{SER}, C_{PAR} and C_{SER} values at 100 and 1000 Hz, is most closely represented by R_{PAR} at 100 Hz. However, the correlation between C_{SER} and $Z_{r,lf}$ observed in Figs. 7 and 8 suggests that C_{SER} measured at 100 Hz might also be used as a surrogate measure for resistivity. Therefore, using the 145 cadaver skin measurements presented in Figs. 6–8, the suitability of using (R_{PAR} A) and (C_{SER}/A) determined at 100 Hz as surrogates for identifying skin samples with acceptable and unacceptable resistivity was explored.

The evaluation scheme is illustrated in Fig. 9. For the selected test value of the area-normalized DC skin resistance (R_{skin} A)$_{test}$, the test value of the surrogate measurement is chosen. For the chosen surrogate test value, the number of skin samples was determined that, according to the area-normalized surrogate measure, was either acceptable or unacceptable. By comparing (R_{skin} A)$_{test}$ to values of ($Z_{r,lf}$ A), assumed to represent (R_{skin} A) for each skin sample, results identified as acceptable according to the surrogate measurements were then categorized as either true acceptable (designated TA), meaning (R_{skin} A) > (R_{skin} A)$_{test}$, or true unacceptable (designated TU), meaning (R_{skin} A) < (R_{skin} A)$_{test}$. Similarly, results identified by the surrogate measurements as unacceptable were categorized as either false acceptable, FA, or false unacceptable, FU, according to (R_{skin} A) compared with (R_{skin} A)$_{test}$. For (R_{PAR} A) as the selected surrogate test measurement, skin samples are deemed acceptable if (R_{PAR} A) P (R_{PAR} A)$_{test}$, and unacceptable if (R_{PAR} A) < (R_{PAR} A)$_{test}$. Since (C_{SER}/A) decreases with increasing skin resistance, skin samples are deemed acceptable if (C_{SER}/A) 6 (C_{SER}/A)$_{test}$, and unacceptable if (C_{SER}/A) > (C_{SER}/A)$_{test}$. The performance results for four surrogate criteria are reported in Table 2 as the percentage of the 145 skin

samples identified as TA, FA, TU or FU for values of $(R_{skin}\ A)_{test}$ between 10 and 36 kΩ-cm^2, which represents the range of previously proposed test values for R_{PAR} or R_{skin}.

The first surrogate criteria in Table 2 is $(R_{PAR}\ A)_{test}$ set equal to $(R_{skin}\ A)_{test}$, which is consistent with the assumption that R_{PAR} measured at 100 Hz is a good estimate of R_{skin}. Because R_{PAR} measured at 100 Hz is generally less than $Z_{r,lf}$ (see Fig. 6), choosing $(R_{PAR}\ A)_{test}$ at 100 Hz to equal $(R_{skin}\ A)_{test}$ is biased toward rejecting acceptable skin samples.

To use (C_{SER}/A) measured at 100 Hz as a surrogate for recognizing skin samples with acceptable and unacceptable resistivity, suitable values for $(C_{SER}/A)_{test}$ must be determined. Assuming the cadaver skin impedance data shown in Fig. 8 are representative of skin samples generally, criteria for $(C_{SER}/A)_{test}$ were estimated by substituting $(R_{skin}\ A)_{test}$ for $(Z_{r,lf}\ A)$ in Eq. (6). Overall, using $(C_{SER}/A)_{test}$ calculated using Eq. (6) as surrogate test criterion for $(R_{skin}\ A)_{test}$ was superior to using $(R_{PAR}\ A)_{test}$ at 100 Hz equal to $(R\text{skin}\ A)\text{test}$.

The following regression of $(R_{PAR}\ A)$ determined at 100 Hz to $(Z_{r,lf}\ A)$,

$$\log(R_{PAR}A) = 0.837\log\left(Z_{r,lf}A\right) + 0.092 \quad r^2 = 0.97 \tag{8}$$

where the units for $(Z_{r,lf}\ A)$ and $(R_{PAR}\ A)$ are kΩ cm^2, should provide an improved criterion for $(R_{PAR}\ A)_{test}$. Specifically, $(R_{PAR}\ A)_{test}$ at 100 Hz is calculated by substituting $(R_{skin}\ A)_{test}$ for $(Z_{r,lf}\ A)$ in Eq. (8). A similar approach was also applied to derive $(R_{PAR}\ A)_{test}$ measured at 1000 Hz from the following regression for $(R_{PAR}\ A)_{test}$ at 1000 Hz to $(Z_{r,lf}\ A)$:

$$\log(R_{PAR}A) = 0.668\log\left(Z_{r,lf}A\right) + 0.053 \quad r^2 = 0.83 \tag{9}$$

Eqs. (8) and (9) are compared with the 145 experimental measurements in Fig. 10. The values of $(R_{PAR}\ A)_{test}$ calculated according to Eqs. (8) and (9) for selected values of $(R_{skin}\ A)_{test}$ are listed in Table 2 along with a performance summary.

Compared with the results for $(R_{PAR}\ A)_{test} = (R_{skin}\ A)_{test}$, applying $(R_{PAR}\ A)_{test}$ calculated from Eq. (8) produced fewer incorrectly identified samples, although more samples were incorrectly identified as acceptable (i.e., FA). Clearly, $(R_{PAR}\ A)$ measured at 1000 Hz is inferior to the other surrogate measurements listed in Table 2 for correctly identifying skin samples with acceptable and unacceptable integrity.

4.5. Comparison to the literature

Eqs. (8) and (9) provide a means of estimating the DC skin resistance that corresponds with the previously proposed test values for R_{PAR} based on LCR databridge measurements. Davies et al. (2004) recommended using $(R_{PAR}\ A)_{test}$ of 25 kΩ cm^2 measured at 100 Hz, which corresponds to $(R_{skin}\ A)_{test}$ equal to about 36 kΩ cm^2 100 Hz, which corresponds to $(R_{skin}\ A)_{test}$ equal to about 36 kΩ cm^2 calculated using Eq. (8). This is not too different from $(R_{skin}\ A)_{test}$ equal to 30 kΩ cm^2, which is estimated for $(R_{PAR}\ A)_{test}$ at 1000 Hz equal to 11 kΩ cm^2 (Fasano et al., 2002). This similarity in $(R_{skin}\ A)_{test}$ values is expected because $(R_{PAR}\ A)_{test}$ in both studies was chosen to match the same value for tritiated water absorption (i.e., 1.5 mg cm^{-2} h^{-1}). Notably, Kasting and Bowman (1990) recommended 35

kΩ cm^2 for $(R_{skin}\ A)_{test}$ based in part on current–voltage behavior in studies of sodium ion absorption in experiments at 37 °C. More recently, 13 kΩ cm^2 and 7 kΩ cm^2 have been suggested for $(R_{PAR}\ A)_{test}$ measured at 100 and 1000 Hz, respectively (Horne et al., 2010); these values, developed to be consistent with a tritiated water absorption of 3.5 mg cm^{-2} h^{-1}, correspond to $(R_{skin}\ A)_{test}$ equal to 16 kΩ cm^2.

From the ratio of urea permeability measured at 39 and 27 °C, Peck et al. (1995) discovered that heat-separated human skin with $(R_{skin}\ A)$ less than 20 kΩ cm^2 at 27 °C, behaved differently than higher resistance skin and like porous Nuclepore membranes. Thus, Peck et al. (1995) selected 20 kΩ cm^2 for $(R_{skin}\ A)_{test}$. This DC resistance criteria would correspond with 15.1 and 8.4 kΩ cm^2 for $(R_{PAR}\ A)_{test}$ determined at 100 and 1000 Hz, respectively or 285 nF/cm^2 for $(C_{SER}/A)_{test}$ measured at 100 Hz.

5. Conclusions

Resistance and capacitance values reported by LCR databridge instruments represent manipulations of the complex impedance and are, therefore, functions of the measurement frequency. With the exception of low impedance skin samples, the R_{SER}, R_{PAR} and C_{PAR} measured at 1000 Hz and R_{SER} and C_{PAR} measured at 100 Hz will generally provide poor estimates of the skin resistivity. Measurements of R_{PAR} and C_{SER} at 100 Hz may be used as surrogate measures for skin resistivity to assess the integrity of human skin samples. While the sensitivity of R_{PAR} measured at low frequency to skin resistance is consistent with results presented in the literature, a surprising result of the present study is that the capacitance C_{SER} measured at low frequency provides an even better surrogate for skin resistivity. One should caution, however, that, depending on the chosen acceptance criteria, some skin may be falsely identified as acceptable or unacceptable.

Acknowledgement

The authors acknowledge support from the National Institute of Occupational Safety and Health (application number 1-R01-OH007493).

Appendix A

The complex impedance of the *R–C* circuit model shown in Fig. 1 is represented by the following equation:

$$Z = R_e + \frac{R_{skin}}{1 + \omega R_{skin} C_{skin}} \tag{A1}$$

from which the real and imaginary parts are determined to be:

$$Z_r = R_e + \frac{R_{skin}}{1 + (\omega R_{skin} C_{skin})^2} \tag{A2}$$

and

$$Z_{\mathrm{j}} = -\frac{\omega R_{\mathrm{skin}}^2 C_{\mathrm{skin}}}{1+(\omega R_{\mathrm{skin}} C_{\mathrm{skin}})^2} \tag{A3}$$

where the radial frequency x is equal to $2\pi f$ for f given in cycles per time.

Although Eqs. (A1), (A2), (A3) capture the essential features of skin impedance measured as a function of frequency, the *R*-CPE circuit model, in which a constant phase element (CPE) replaces the capacitor shown in Fig. 1, provides better quantitative agreement with experimental data (Hirschorn et al., 2010; Kontturi and Murtomaki, 1994; Yamamoto and Yamamoto, 1976a, 1976b, 1981).

The complex impedance of the *R*-CPE model circuit is more complicated than the *R*–*C* model circuit because the impedance of a CPE depends on two parameters, Q and α, rather than just one (the capacitance, C_{skin}) for a capacitor. For the *R*-CPE model circuit, the PAR and SER modes for R and C are described by the following four equations:

$$R_{\mathrm{PAR}} = \frac{(R+R_{\mathrm{e}})^2 + (RR_eQ\omega^{\alpha})^2 + 2(R+R_{\mathrm{e}})QRR_{\mathrm{e}}\omega^{\alpha}\cos\left(\frac{\alpha\pi}{2}\right)}{R+R_{\mathrm{e}}+R_{\mathrm{e}}(QR\omega^{\alpha})^2 + (R+2R_{\mathrm{e}})QR\omega^{\alpha}\cos\left(\frac{\alpha\pi}{2}\right)} \tag{A4}$$

$$R_{\mathrm{SER}} = Z_{\mathrm{r}} = R_{\mathrm{e}} + \frac{R+R^2Q\omega^{\alpha}\cos\left(\frac{\alpha\pi}{2}\right)}{1+(RQ\omega^{\alpha})^2+2RQ\omega^{\alpha}\cos\left(\frac{\alpha\pi}{2}\right)} \tag{A5}$$

$$C_{\mathrm{PAR}} = \frac{Y_{\mathrm{j}}}{\omega} = \frac{QR^2\omega^{(\alpha-1)}\sin\left(\frac{\alpha\pi}{2}\right)/(R+R_{\mathrm{e}})}{R_{\mathrm{e}}+R+\frac{(RQR_{\mathrm{e}}\omega^{\alpha})^2}{R+R_{\mathrm{e}}}+2QRR_{\mathrm{e}}\omega^{\alpha}\cos\left(\frac{\alpha\pi}{2}\right)} \tag{A6}$$

and

$$C_{\mathrm{SER}} = -\frac{1}{Z_{\mathrm{j}}\omega} = \frac{1+(RQ\omega^{\alpha})^2+2RQ\omega^{\alpha}\cos\left(\frac{\alpha\pi}{2}\right)}{R^2Q\omega^{(\alpha+1)}\sin\left(\frac{\alpha\pi}{2}\right)} \tag{A7}$$

The effective capacitance of an *R*-CPE model circuit of skin can be estimated using Eq. (7) from the characteristic frequency, defined here as the frequency at which the negative of the imaginary part of the impedance is at its maximum value (Orazem and Tribollet, 2008). It follows that this definition of the effective skin capacitance ($C_{\mathrm{skin,eff}}$) is related to α and Q as follows:

$$C_{\mathrm{skin,eff}} = Q^{1/\alpha}R_{\mathrm{skin}}^{(1-\alpha)/\alpha} \tag{A8}$$

As described by Hirschorn et al. (2010), Eq. (A8) is in agreement with the development presented by Hsu and Mansfeld (2001) and used by Oh and Guy (1994a, 1994b) to estimate the capacitance of human skin when α is close to one.

References

Barel AO, Clarys P, 2006. Measurement of epidermal capacitance. In: Serup J, Jemec GBE, Grove GL (Eds.), Handbook of Non-Invasive Methods and the Skin, second ed. Taylor & Francis, Boca Raton, FL.

Curdy C, Kalia YN, Guy RH, 2001. Non-invasive assessment of the effects of iontophoresis on human skin in-vivo. J. Pharm. Pharmacol 53, 769–777. [PubMed: 11428652]

Curdy C, Naik A, Kalia YN, Alberti I, Guy RH, 2004. Non-invasive assessment of the effect of formulation excipients on stratum corneum barrier function in vivo. Int. J. Pharm 271, 251–256. [PubMed: 15129992]

Davies DJ, Ward RJ, Heylings JR, 2004. Multi-species assessment of electrical resistance as a skin integrity marker for in vitro percutaneous absorption studies. Toxicol. In Vitro 18, 351–358. [PubMed: 15046783]

DeNuzzio JD, Berner B, 1990. Electrochemical and iontophoretic studies of human skin. J. Controlled Release 11, 105–112.

Fasano WJ, Hinderliter PM, 2004. The Tinsley LCR Databridge Model 6401 and electrical impedance measurements to evaluate skin integrity in vitro. Toxicol. In Vitro 18, 725–729. [PubMed: 15251192]

Fasano WJ, Manning LA, Green JW, 2002. Rapid integrity assessment of rat and human epidermal membranes for in vitro dermal regulatory testing: correlation of electrical resistance with tritiated water permeability. Toxicol. In Vitro 16, 731–740. [PubMed: 12423657]

Franz TJ, Lehman PA, 1990. The use of water permeability as a means of validation for skin integrity in vitro percutaneous absorption studies. J. Invest. Dermatol 94, 525.

Gabard B, Clayrs P, Barel AO, 2006. Comparison of commercial electrical measurement instruments for assessing the hydration state of the stratum corneum. In: Serup J, Jemec GBE, Grove GL (Eds.), Handbook of Non-Invasive Methods and the Skin, second ed. Taylor & Francis, Boca Raton, FL.

Heylings JR, 2009. Personal communication, October 13.

H. Tinsley & Co. 1996. 6401 LCR Databridget Users Manual Surrey, England.

Heylings JR, Esdaile DJ, 2007. Percutaneous absorption of pesticides. In: Roberts MS, Walters KA (Eds.), Dermal Absorption and Toxicity Assessment, second ed. Informa Healthcare, New York, pp. 575–591.

Hirschorn B, Orazem ME, Tribollet B, Vivier V, Frateur I, Musiani M, 2010. Determination of effective capacitance and film thickness from constant-phase-element parameters. Electrochim. Acta 55, 6218–6227.

Horne A, Blackstock C, Roper CS, 2010. Evaluation of electrical resistance for use as a rapid method for human skin barrier integrity assessment in the flow through diffusion cell, Proceedings of the Skin Forum, 11th Annual Meeting. Edinburgh, Scotland.

Hsu CH, Mansfeld F, 2001. Technical note: concerning the conversion of the constant phase element parameter Y0 into a capacitance. Corrosion 57, 747–748.

International Programme on Chemical Safety (IPCS), 2006. Dermal Absorption, Environmental Health Criteria 235 World Health Organization, Geneva.

Kalia YN, Nonato LB, Lund CH, Guy RH, 1998. Development of skin barrier function in premature infants. J. Invest. Dermatol 111, 320–326. [PubMed: 9699737]

Kalia YN, Pirot F, Guy RH, 1996. Homogeneous transport in a heterogeneous membrane: water diffusion across human stratum corneum *in vivo*. Biophys. J 71, 2692–2700. [PubMed: 8913606]

Kasting GB, Bowman LA, 1990. DC electrical properties of frozen, excised human skin. Pharm. Res 7, 134–143. [PubMed: 2308893]

Kasting GB, Filloon TG, Francis WR, Meredith MP, 1994. Improving the sensitivity of in vitro skin penetration experiments. Pharm. Res 11, 1747–1754. [PubMed: 7899239]

Kontturi K, Murtomaki L, 1994. Impedance spectroscopy in human skin. A refined model. Pharm. Res 11, 1355–1357. [PubMed: 7816769]

Membrino MA, Orazem ME, Scott E, Phipps JB, 1997. Electrochemical impedance measurements for characterization of ion transport pathways in skin. Minutes: Transdermal Administration: A Case Study. Iontophoresis Editions de Sante, Paris, France. pp. 313–317.

Nicander I, Åberg P, Ollmar S, 2006. Bioimpedance as a noninvasive method for measuring changes in skin. In: Serup J, Jemec GBE, Grove GL (Eds.), Handbook of Non-Invasive Methods and the Skin, second ed. Taylor & Francis, Boca Raton, FL.

OECD, 2004a. Guideline for Testing of Chemicals. Guideline 428: Skin Absorption: In Vitro Method (Original Guideline, adopted 13th April 2004).

OECD, 2004b. OECD Guideline for the Testing of Chemicals. Guideline 430: In Vitro Skin Corrosion: Transcutaneous Electrical Resistance Test (TER).

Oh SY, Leung L, Bommannan D, Guy RH, Potts RO, 1993. Effect of current, ionic strength and temperature on the electrical properties of skin. J. Controlled Release 27, 115–125.

Oh SY, Guy RH, 1994a. Effect of enhancers on the electrical properties of skin: The effect of azone and ethanol. J. Kor. Pharm. Sci 24, S41–S47.

Oh SY, Guy RH, 1994b. The effect of oleic acid and propylene glycol on the electrical properties of skin. J. Kor. Pharm. Sci 24, 281–287.

Orazem ME, Tribollet B, 2008. Electrochemical Impedance Spectroscopy Wiley-Interscience, Hoboken, NJ.

Peck KD, Ghanem AH, Higuchi WI, 1994. Hindered diffusion of polar molecules through and effective pore radii estimates of intact and ethanol treated human epidermal membrane. Pharm. Res 11, 1306–1314. [PubMed: 7816761]

Peck KD, Ghanem AH, Higuchi WI, 1995. The effect of temperature upon the permeation of polar and ionic solutes through human epidermal membrane. J. Pharm. Sci 84, 975–982. [PubMed: 7500283]

Poon CS, Choy TTC, 1981. Frequency dispersions of human-skin dielectrics. Biophys. J 34, 135–147. [PubMed: 7213928]

Rosell J, Colominas J, Riu P, Pallasareny R, Webster JG, 1988. Skin impedance from 1 Hz to 1 MHz. IEEE Trans. Biomed. Eng 35, 649–651. [PubMed: 3169817]

Scott RC, Batten PL, Clowes HM, Jones BK, Ramsey JD, 1992. Further validation of an in vitro method to reduce the need for in vivo studies for measuring the absorption of chemicals through rat skin. Fundam. Appl. Toxicol 19, 484–492. [PubMed: 1426705]

Scott RC, Corrigan MA, Smith F, Mason H, 1991. The influence of skin structure on permeability: an intersite and interspecies comparison with hydrophilic penetrants. J. Invest. Dermatol 96, 921–925. [PubMed: 1904468]

Tagami H, 2006. Epidermal hydration: measurement of high-frequency electrical conductance. In: Serup J, Jemec GBE, Grove GL (Eds.), Handbook of Non-Invasive Methods and the Skin, second ed. Taylor & Francis, Boca Raton, FL.

White EA, 2011. PhD Thesis. Colorado School of Mines, Golden, Colorado.

Yamamoto T, Yamamoto Y, 1976a. Dielectric constant and resistivity of epidermal stratum corneum. Med. Biol. Eng. Compu 14, 494–500.

Yamamoto T, Yamamoto Y, 1976b. Electrical properties of the epidermal stratum corneum. Med. Biol. Eng. Compu 14, 151–158.

Yamamoto T, Yamamoto Y, 1981. Non-linear electrical-properties of skin in the low-frequency range. Med. Biol. Eng. Compu 19, 302–310.

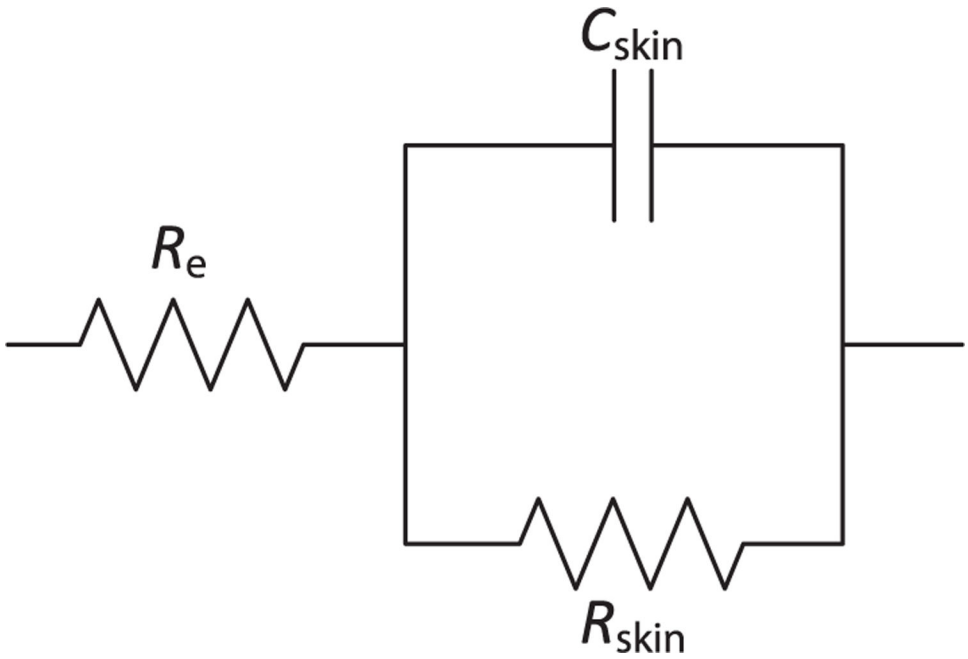

Fig. 1.
A simple *R–C* circuit model of skin.

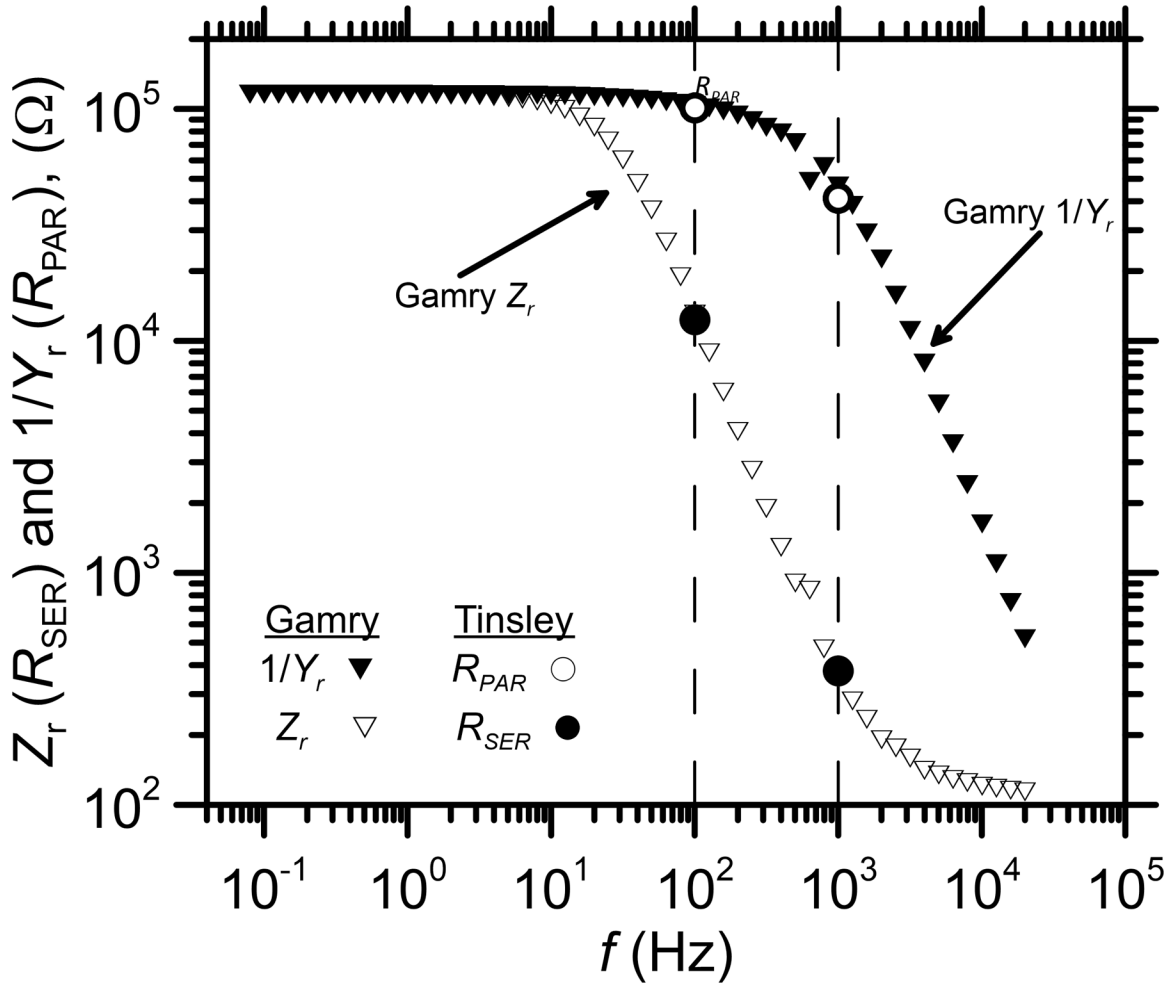

Fig. 2.

R_{PAR} and R_{SER} measured by the Tinsley LCR databridge at 100 and 1000 Hz compared with Z_r and 1/Y_r spectra measured by the Gamry potentiostat for the dummy cell (R_e = 100 Ω, R_{skin} = 115 kΩ, C_{skin} = 47 nF).

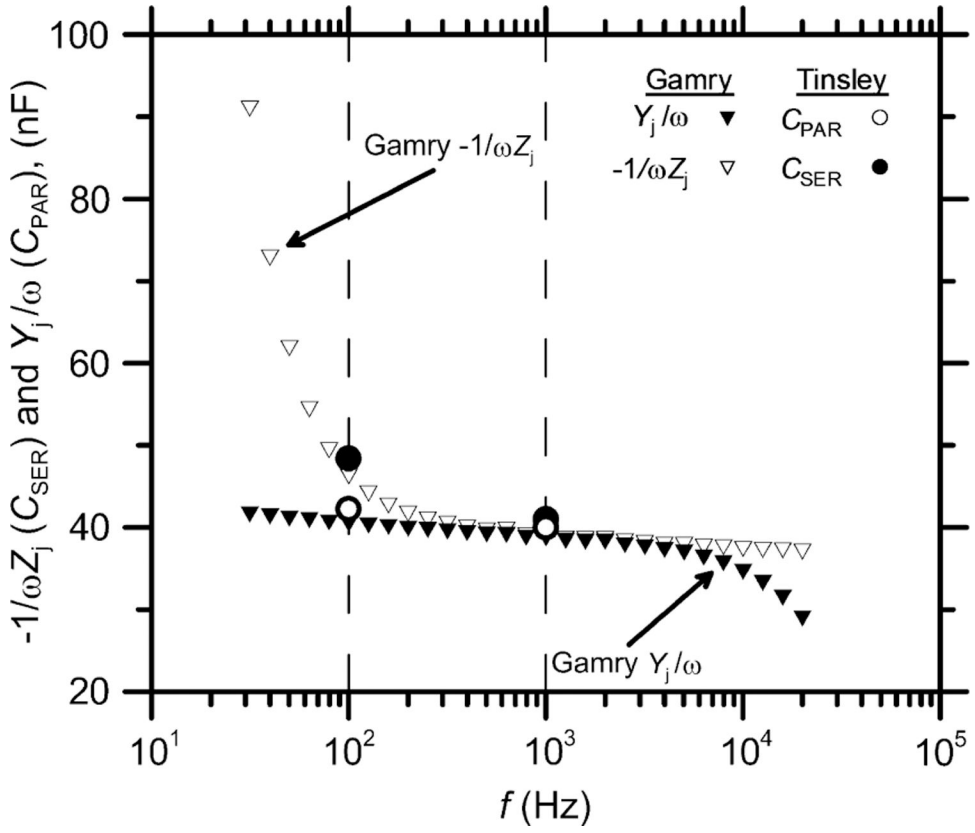

Fig. 3.

C_{PAR} and C_{SER} measured by the Tinsley LCR databridge compared with Y_j/ω and-$1/\omega Z_j$ spectra measured by the Gamry potentiostat for the dummy cell (R_e = 100 Ω, R_{skin} = 115 k Ω, C_{skin} = 47 nF).

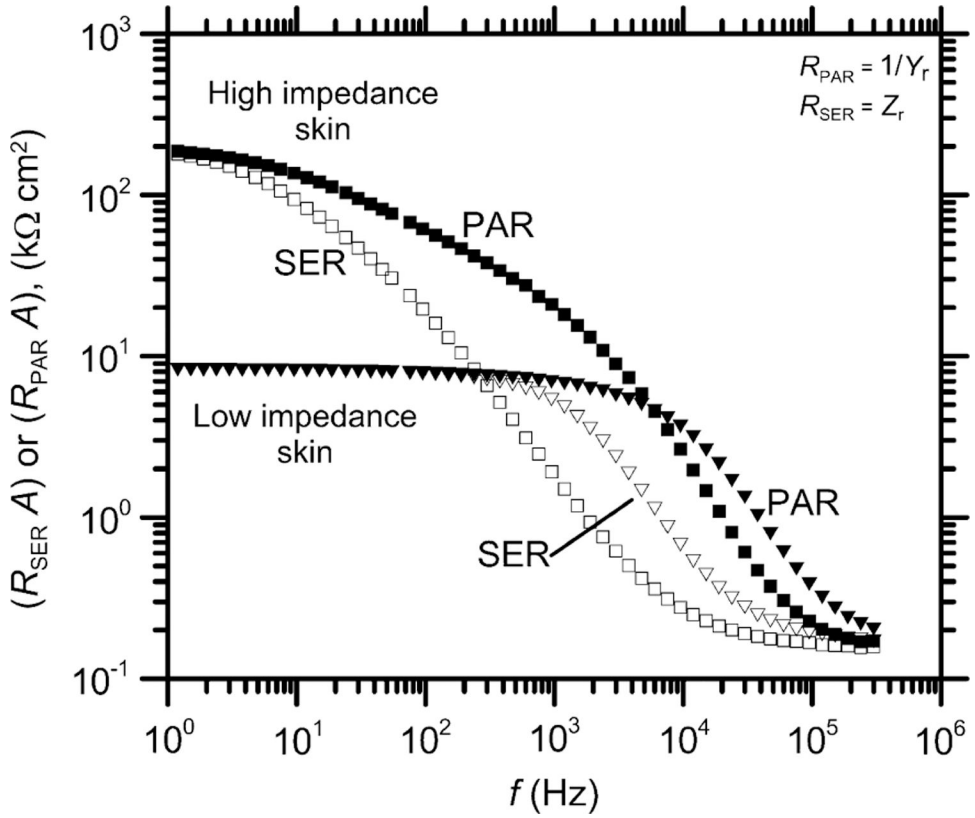

Fig. 4.

Area-normalized values of R_{SER} (open symbols) and R_{PAR} (filled symbols) calculated from the complex impedance measured with the Gamry potentiostat as a function of frequency for a high impedance skin sample (squares) and a low impedance skin sample (triangles).

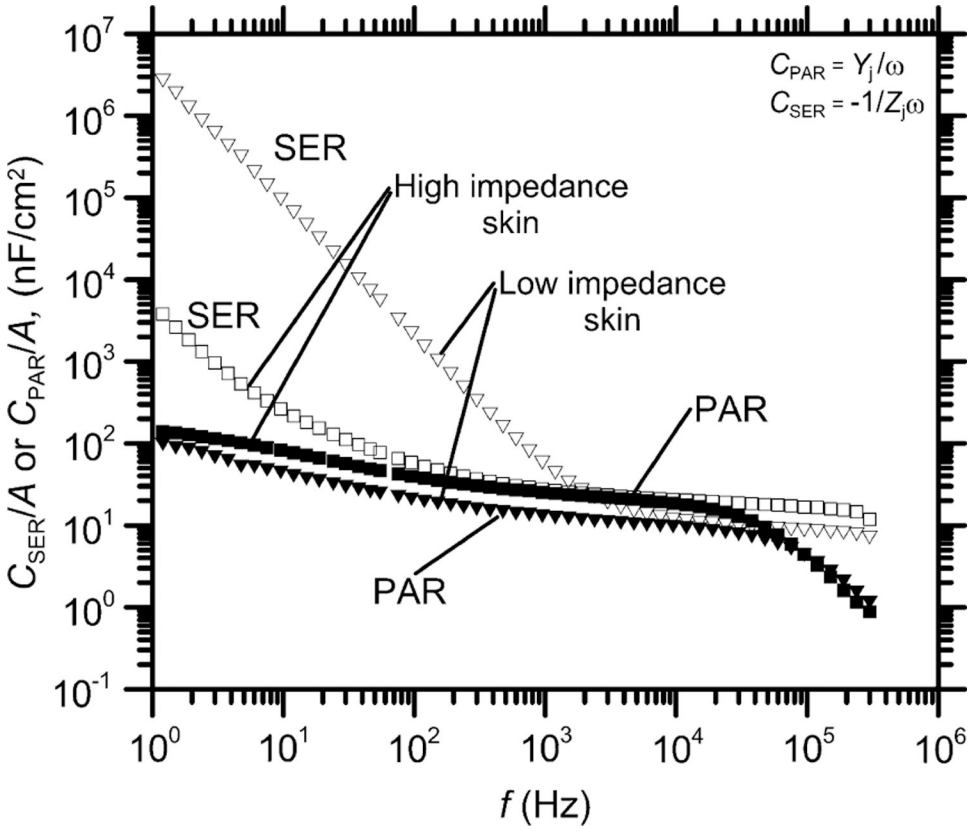

Fig. 5.

Area normalized values of C_{SER} (open symbols) and C_{PAR} (filled symbols) calculated from the complex impedance measured with the Gamry potentiostat as a function of frequency for a high impedance skin sample (squares) and a low impedance skin sample (triangles).

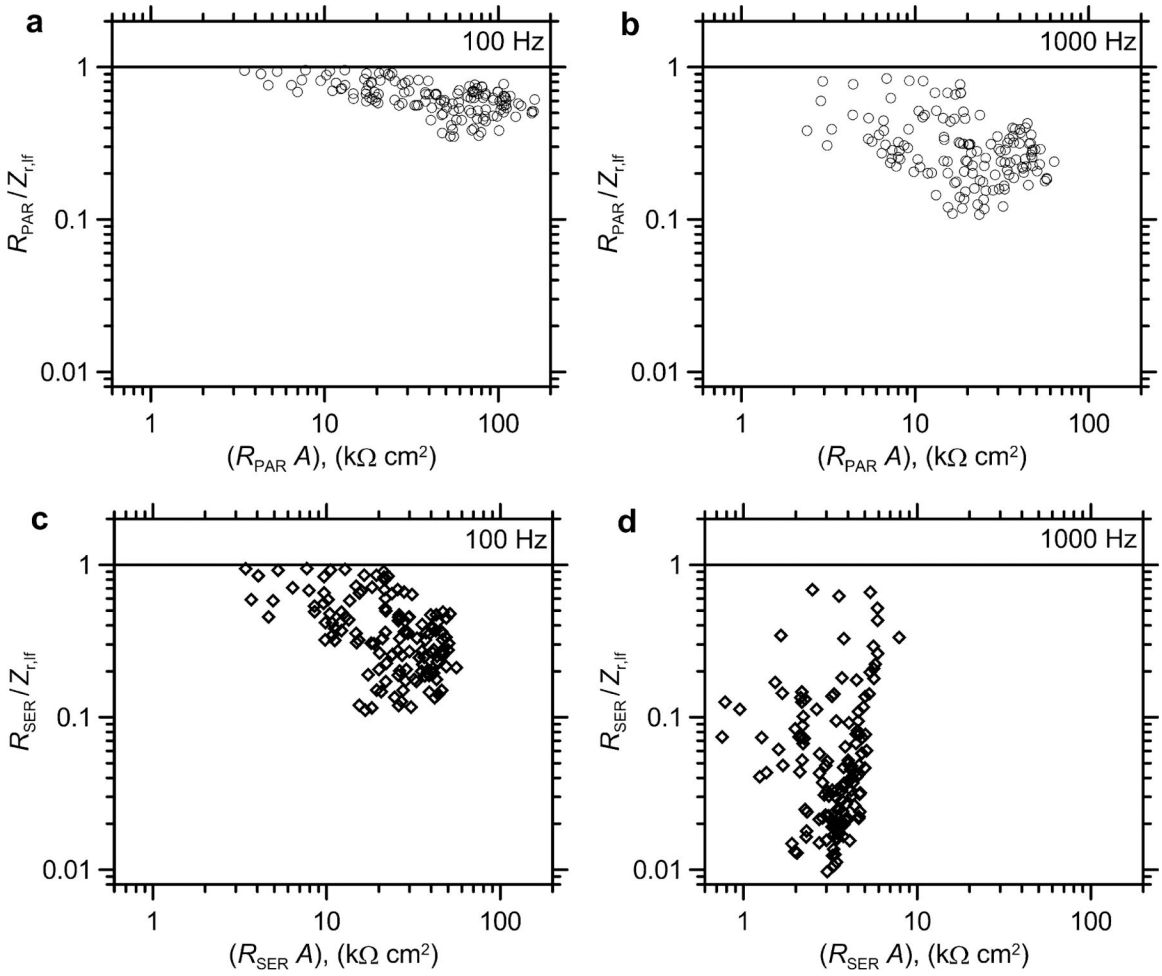

Fig. 6.

Ratios of R_{PAR} and R_{SER} to the low frequency real impedance ($Z_{r,lf} \cong R_{skin}$) plotted as a function of R_{PAR} and R_{SER}, respectively for 145 samples of human cadaver skin measured at 100 or 1000 Hz.

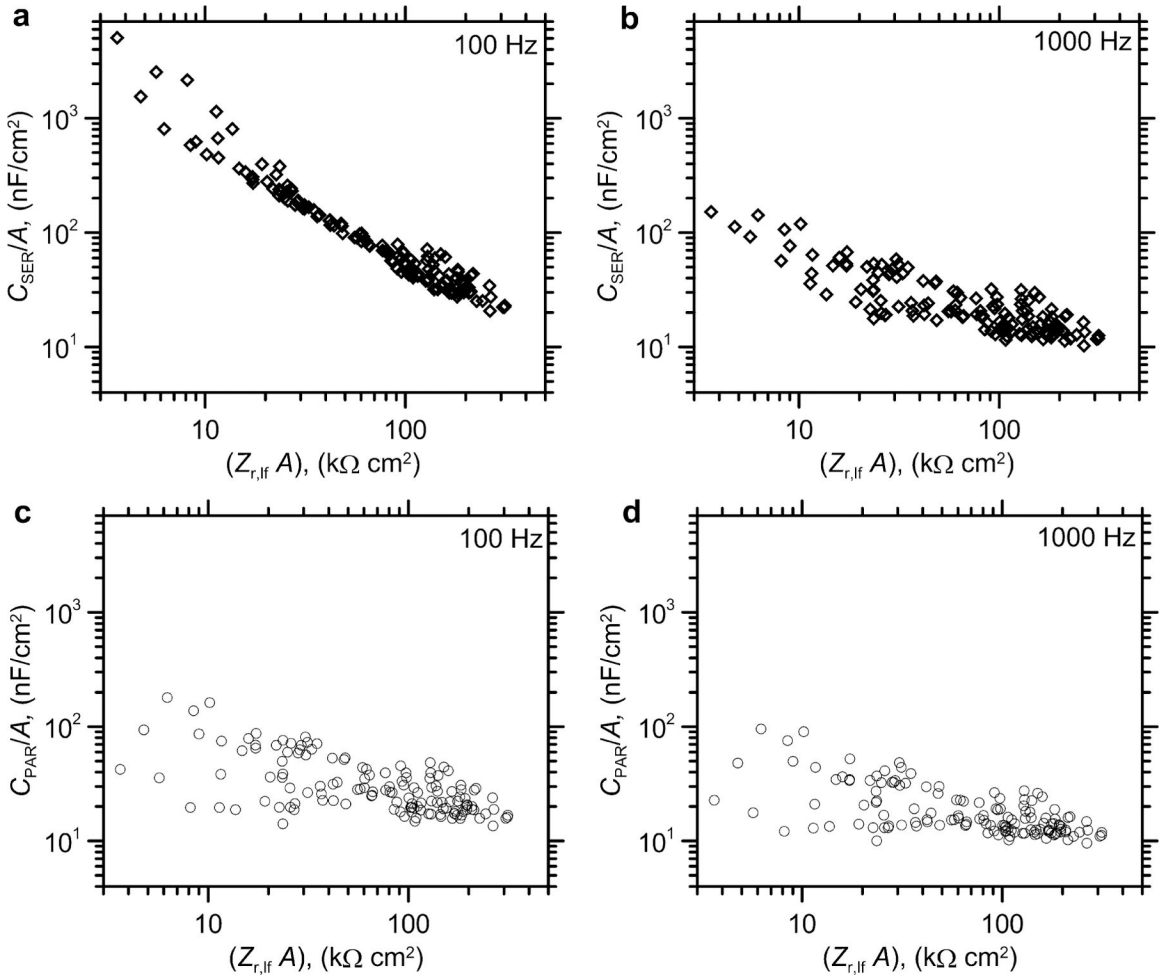

Fig. 7.

Area-normalized values of C_{SER} and C_{PAR} calculated from the complex impedance of 145 cadaver skin samples measured using the Gamry potentiostat at either 100 or 1000 Hz and plotted as a function of ($Z_{r,lf}\ A$).

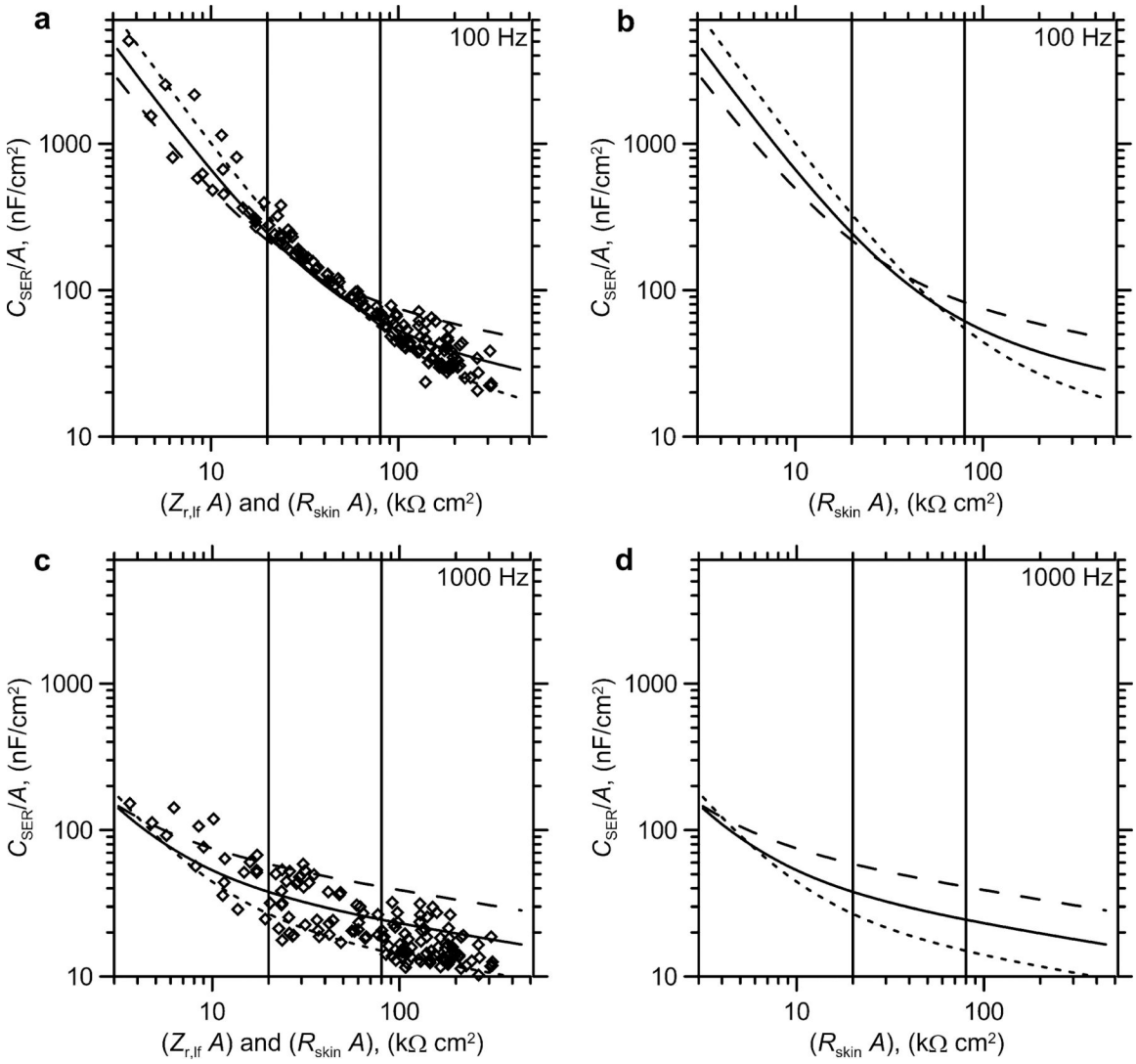

Fig. 8.

Area-normalized values of C_{SER} calculated from the complex impedance of 145 cadaver skin samples measured using the Gamry potentiostat plotted as a function of the $Z_{r,lf}$ compared with C_{SER}/A predicted by the *R*-CPE model circuit plotted as a function of R_{skin} for the mean value of $C_{skin,eff}$/A (solid curve) plus and minus one standard deviation (long and short dashed curves respectively) assuming a log mean distribution of $C_{skin,eff}$/A for the 145 skin samples shown in Figs. 6 and 7: data compared with model at 100 Hz (a) and 1000 Hz (c); and model alone at 100 Hz (b) and 1000 Hz (d).

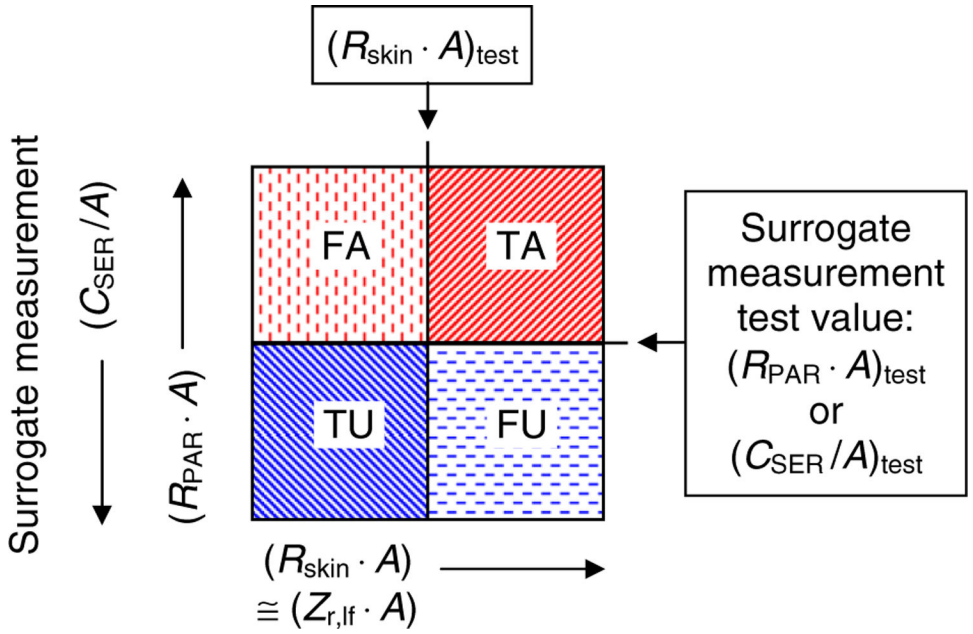

Fig. 9.

Schematic diagram illustrating the scheme for evaluating surrogate measurements for testing skin integrity.

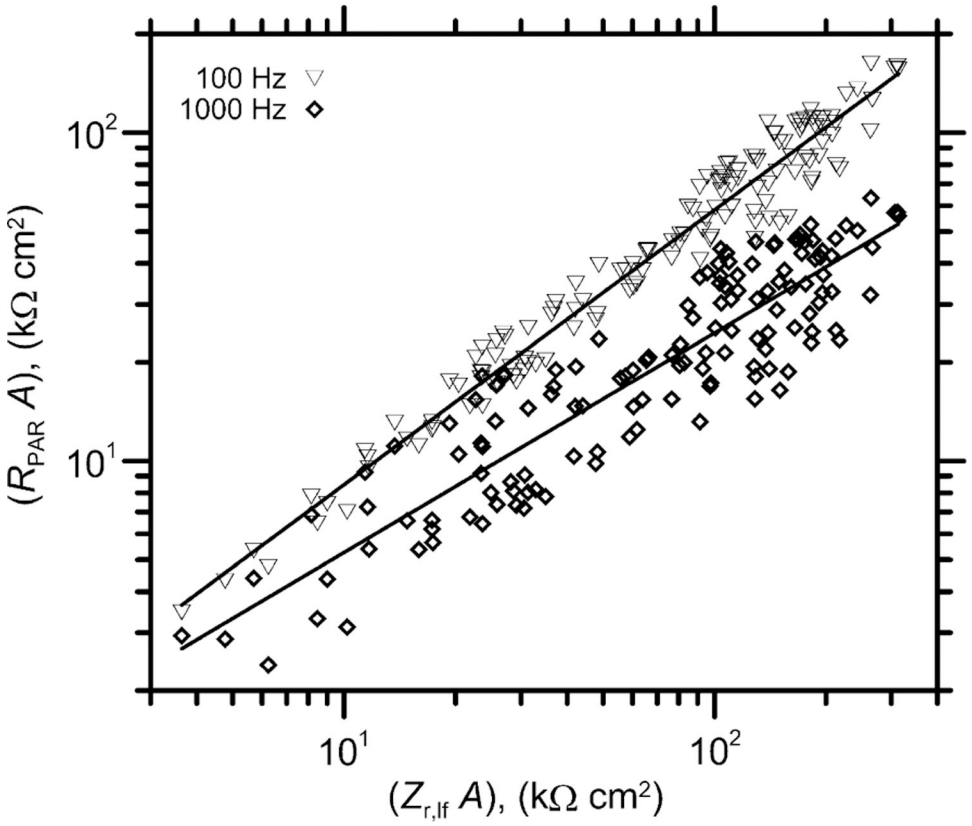

Fig. 10.

Area-normalized values of R_{PAR} calculated from the complex impedance of 145 cadaver skin samples measured at 100 Hz and 1000 Hz using the Gamry potentiostat plotted as a function of the ($Z_{r,lf}$ A). The solid lines were determined by linear regression and correspond to Eqs. (8) and (9) for the 100 Hz and 1000 Hz measurements, respectively.

Table 1

Equations for the PAR and SER modes of R and C for the R–C model circuit shown in Fig. 1.

	PAR	SER
R	$R_{\mathrm{PAR}} = \frac{1}{Y_{\mathrm{r}}} = \frac{R_{\mathrm{skin}}\left[\left(1+\frac{R_{\mathrm{e}}}{R_{\mathrm{skin}}}\right)^2 + (\omega R_{\mathrm{e}} C_{\mathrm{skin}})^2\right]}{R_{\mathrm{e}} R_{\mathrm{skin}} (\omega C_{\mathrm{skin}})^2 + 1 + \frac{R_{\mathrm{e}}}{R_{\mathrm{skin}}}}$	$R_{\mathrm{SER}} = Z_{\mathrm{r}} = R_{\mathrm{e}} + \frac{R_{\mathrm{skin}}}{1 + (\omega R_{\mathrm{skin}} C_{\mathrm{skin}})^2}$
C	$C_{\mathrm{PAR}} = \frac{Y_{\mathrm{j}}}{\omega} = \frac{C_{\mathrm{skin}}}{\left(1+\frac{R_{\mathrm{e}}}{R_{\mathrm{skin}}}\right)^2 + (\omega R_{\mathrm{e}} C_{\mathrm{skin}})^2}$	$C_{\mathrm{SER}} = \frac{1}{-Z_j \omega} = C_{\mathrm{skin}} + \frac{1}{\omega^2 R_{\mathrm{skin}}^2 C_{\mathrm{skin}}}$

Toxicol In Vitro. Author manuscript; available in PMC 2022 August 23.

Table 2

Performance of (R_{PAR} A) at 100 Hz and 1000 Hz and (C_{SER}/A) at 100 Hz as surrogate criteria for (R_{skin} A) in testing skin integrity[a].

Surrogate Criterion			Test value[b]	$(R_{skin}\ A)_{test}$ kΩ cm^2	TA	TU	FA	FU
f (Hz)	Quantity	Relationship of test value to $(R_{skin}\ A)_{test}$ [b]						
100	(R_{PAR} A)	$(R_{PAR}\ A)_{test} = (R_{skin}\ A)_{test}$	10	10	93.8	5.5	0.0	0.7
			15	15	85.5	10.3	0.0	4.1
			20	20	75.2	13.8	0.0	11.0
			25	25	68.3	20.7	0.0	11.0
			30	30	64.1	26.9	0.0	9.0
			36	36	60.0	32.4	0.0	7.6
100	(C_{SER}/A)	Eq. (6): $\log (C_{SER}/A)_{test} = -1.07 \log(R_{skin}\ A)_{test} + 3.85$	598	10	92.4	4.8	0.7	2.1
			387	15	89.0	9.0	1.4	0.7
			285	20	84.8	13.1	0.7	1.4
			224	25	76.6	19.3	1.4	2.8
			185	30	73.1	26.2	0.7	0.0
			152	36	67.6	32.4	0.0	0.0
100	(R_{PAR} A)	Eq. (8): $\log (R_{PAR}\ A)_{test} = 0.837 \log(R_{skin}\ A)_{test} + 0.092$	8.5	10	93.8	5.5	0.0	0.7
			11.9	15	89.0	9.7	0.7	0.7
			15.1	20	84.8	13.1	0.7	1.4
			18.3	25	76.6	17.2	3.4	2.8
			21.3	30	68.3	24.1	2.8	4.8
			24.8	36	67.6	31.7	0.7	0.0
1000	(R_{PAR} A)	Eq. (9): $\log (R_{PAR}\ A)_{test} = 0.668 \log(R_{skin}\ A)_{test} + 0.053$	5.3	10	93.8	4.8	0.7	0.7
			6.9	15	85.5	8.3	2.1	4.1
			8.4	20	77.9	11.7	2.1	8.3
			9.7	25	71.0	15.2	5.5	8.3
			11.0	30	66.2	19.3	7.6	6.9
			12.4	36	64.8	26.9	5.5	2.8

[a]Results are reported as the percentage of the 145 skin samples that are identified by the surrogate criterion as acceptable in agreement (TA = true acceptable) or disagreement (FA = false acceptable) with (R_{skin} A) or that are identified by the surrogate criterion as unacceptable in agreement (TU = true unacceptable) or disagreement (FU = false unacceptable) with (R_{skin} A). For (R_{skin} A) and (R_{PAR} A), acceptable skin must exceed the test value; for (C_{SER}/A) acceptable skin must be less than the test value.

[b] Test value of the surrogate measurement in units of kΩ cm^2 for $(R_{PAR} \cdot A)_{test}$ and nF/cm^2 for $(C_{SER}/A)_{test}$.